Ocean & Sea Ice SAF

Global Sea Ice Concentration Reprocessing

Product User Manual

Product OSI-409

Document version: 1.3

Data set version: 1.1

October 2011

Steinar Eastwood, met.no
Kristian Rune Larsen, DMI
Thomas Lavergne, met.no
Esben Nielsen, DMI
Rasmus Tonboe, DMI

The EUMETSAT
Network of
Satellite Application
Facilities

OSI SAF
Ocean and Sea Ice

Documentation Change Record

Document version	Data set version	Software version	Date	Change Description
V 1.0	V 1.0	V 4.0	14.01.2010	First version.
V 1.1	V 1.0	V 4.0	30.03.2010	Updates after DRI review.
V 1.2	V 1.1	V 4.0	23.06.2011	The uncertainties have been re-calculated with a corrected and re-implemented algorithm. Added 2008 -10.2009.
V 1.3	V 1.1	V 4.0	21.10.2011	Updated after DRI2 review

The software version number gives the corresponding version of the OSI SAF High Latitude software chain which was used to produce the reprocessing data set.

CONTENTS

1. Introduction

1.1 OSI SAF overview

The Ocean and Sea Ice Satellite Application Facility, OSI SAF, is a EUMETSAT project that started in 1997. The OSI SAF is a part of the EUMETSAT distributed ground segment for production of operational near real time value added satellite products. The OSI SAF delivers a range of air-sea interface products, namely: sea ice characteristics, sea surface temperature, radiative fluxes and wind. The sea ice products are sea ice concentration, sea ice edge, sea ice type and sea ice drift.

The OSI SAF project is managed by CMS, Meteo-France. The sea ice products are produced at the OSI SAF High Latitude processing facility under the responsibility of the Norwegian Meteorological Institute, operated jointly by the Norwegian and Danish Meteorological Institutes.

1.2 Sea ice concentration reprocessing project

Since the start of the operational production of sea ice products in 2002 the growing user group has brought more focus on expanding the available data set. It was therefore decided to reprocess historical passive microwave data to extend the OSI SAF sea ice data set. This effort was started in 2006 as a part time EUMETSAT visiting scientist activity in collaboration with the UK Met Office. The goal was to reprocess the SSM/I data record. A collaboration was also established with NSIDC to include the SMMR data record in the project, and an EUMETSAT visiting scientist project was set up for this task. These two Visiting Scientist projects initiated the OSI SAF reprocessing and produced a first version of reprocessing data set based on the SSM/I data. Later further improvements have been implemented before the current version was finished.

This reprocessing product fulfills the requirement OSI-PRD-PRO-205 in the OSI SAF Product Requirement Document [RD.1]. No validation results are presented in this document. The validation results are presented in a separate validation report [RD.2].

1.3 Data set version

This product user manual describes version 1.1 of the OSI SAF reprocess sea ice concentration data set, which was released in October 2011.

1.4 Ownership and copyright of data

The OSI SAF reprocessed sea ice concentration data set has been produced under responsibility of Norwegian Meteorological Institute and Danish Meteorological Institute. The ownership and copyrights of the data set belongs to EUMETSAT. The data set is distributed freely, but EUMETSAT must be acknowledged when using the data. EUMETSAT's copyright credit must be shown by displaying the words "copyright (year) EUMETSAT" on each of the products used.

1.5 Acknowledgment

We would like to thank John Stark (previously at the UK Met Office) for his effort as a visiting scientist under the OSI SAF IOP-SG06-VS01 Visiting Scientist project. His efforts are documented in Stark (2008).

We would also like to thank Walt Meier and Jeff Smith at NSIDC for their cooperation and effort during the OSI SAF CDOP-SG01-VS03 Visiting Scientist project. Their work is documentation in Meier (2008).

1.6 Glossary

ASCII	American Standard Code for Information Interchange
CMS	Centre de Météorologie Spatiale
CDL	network Common data form Description Language
CDOP	Continuous Development and Operations Phase (OSI SAF project)
CF	Climate and Forecast (Metadata Conventions)
DMI	Danish Meteorological Institute
DMSP	Defense Meteorological Satellite Program
EASE	Equal-Area Scalable Earth
ECMWF	European Centre for Medium range Weather Forecast
ERA	ECMWF Re-Analysis
FTP	File Transfer Protocol
EUMETSAT	European Organisation for the Exploitation of Meteorological Satellites
GCMD	Global Change Master Directory
met.no	Norwegian Meteorological Institute
NASA	National Aeronautics and Space Administration
NetCDF	Network Common Data Form
NSIDC	National Snow and Ice Data Center
NWP	Numerical Weather Prediction
OSI SAF	Ocean and Sea Ice Satellite Application Facility
RTM	Radiative Transfer Model
RSS	Remote Sensing Systems
SAR	Synthetic Aperture Radar
SMMR	Scanning Multichannel Microwave Radiometer
SSM/I	Special Sensor Microwave/Imager
TUD	Technical University of Denmark

1.7 Reference Documents

[RD.1] OSI SAF CDOP Product Requirement Document, v1.2.

[RD.2] OSI SAF Sea Ice Concentration Reprocessing Product Validation Report.

[RD.3] OSI SAF IOP-SG06-VS01 report (Stark, 2008).

[RD.4] OSI SAF CDOP-SG01-VS03 report (Meier, 2008).

[RD.5] Adaption of SAFOSI sea ice processing system to southern hemisphere (Toudal, 2006).

2. Input data

This chapter describes the main input data that have been used for the OSI SAF sea ice concentration reprocessing.

2.1 SMMR

The Scanning Multichannel Microwave Radiometer (SMMR) instrument on board the Nimbus 7 satellite operated from October 1978 to August 1987 (Gloersen et al., 1992). The instrument was operated only every second day due to power supply limitations. The instrument had 10 channels from the six Dicke radiometers at five frequencies (6.6, 10.7, 18.0, 21.0, 37.0 GHz) and vertical and horizontal polarization. The scanning across track was ensured by tilting the reflector from side to side while maintaining constant incidence angle on the ground of about 50°. The scan track on the ground formed a 780 km wide arc in front of the satellite (Gloersen and Barath, 1977). Because of the satellite orbit inclination and swath width there is no coverage poleward of 84°. The SMMR instrument is further described in http://nsidc.org/data/docs/daac/smmr_instrument.gd.html and the brightness temperature data and the initial formatting of the data are described in Meier (2008).

Frequency (GHz)	Polarizations	Field of view	
		Along-track	Cross-track
6.6	H,V	148 km	95 km
10.7	H,V	91 km	59 km
18.0	H,V	55 km	41 km
21.0	H,V	46 km	30 km
37.0	H,V	27 km	18 km

Table 1: Characteristics of the Nimbus 7 SMMR channels (Gloersen and Barath, 1977).

2.2 SSM/I

The Special Sensor Microwave/Imager (SSM/I) sensors on bord the Defence Meteorological Satellite Program (DMSP) started its record with the F08 satellite on 9. July 1987 shortly before the SMMR ceased to operate on 20. August 1987. The different SSM/I instrument records are summarised in table 2. The SSM/I is a total power radiometer with a conical scan measuring the upwelling radiation from the Earth at a constant incidence angle of about 50deg at 7 different channels. The channels are summarised in table 3. The swath width is about 1400km.

The Special Sensor Microwave/Imager (SSM/I) data set used for this reprocessing was purchased by EUMETSAT from Remote Sensing Systems (RSS) and covers the whole period of available satellites with SSMI/I instruments from 1987 to 2009. We have used the version 6 of the RSS SSM/I data set. The different satellites and covered periods are listed in Table 2.

The SSM/I data were received as antenna temperatures from RSS. These antenna temperatures were converted to brightness temperatures (Tb's) using a software provided by RSS, as described in chapter 4.1.1.

The SSM/I instrument have five low frequency channels similar to SMMR. In addition, two higher frequency channels with twice the sampling rate are available on the SSM/I. The characteristics of these channels are listed in Table 3. The 85GHz channels had a

malfunction on F08, so they are only useful starting with the F11 satellite. The F10 has not been used because they are more noisy than F11 and were not needed for a complete coverage.

Satellite	Period covered
F08	Jul 1987 – Dec 1991
F11	Dec 1991 – May 2000
F13	Dec 1995 – Oct 2009
F14	May 1997 – Aug 2008
F15	Dec 1999 – Oct 2009

Table 2: The different satellite missions carrying the SSM/I instrument and the periods they cover.

Frequency (GHz)	Polarizations	Footprint size	
		Along-track	Cross-track
19.35	H,V	69 km	43 km
22.235	V	50 km	40 km
37.0	H,V	37 km	28 km
85.5	H,V	15 km	13 km

Table 3: Characteristics of the different SSM/I channels (from Wentz, 1991).

The RSS SSM/I version 6 data set incorporates geolocation correction, sensor calibration and quality control procedures, as well as inter calibration between the different satellites from overlapping periods. These procedures are documented in the RSS SSM/I User's Manuals (Wentz, 1991; Wentz, 1993; Wentz, 2006).

The RSS SSM/I data set is constrained with a license for use and distribution, and the brightness temperatures on swath format used in the OSI SAF reprocessing product can therefore not be distributed.

2.3 ECMWF NWP

The brightness temperatures (Tb) are corrected explicitly for wind roughening over open water and water vapor in the atmosphere prior to the calculation of ice concentration. The correction is using a radiative transfer model function (RTM) and NWP data. The model function used for correction of the SMMR and SSM/I Tbs using ECMWF NWP input is denoted by (Wentz, 1983):

$$Tb = f(Ts, U^*, V, L, Ta) \quad , \qquad \text{(Eq. 1)}$$

where Ts is the physical surface temperature, U^* is the sea surface wind friction velocity, V is the integrated atmospheric water vapor column, L is the atmospheric liquid water column, and Ta is the surface (2 m) air temperature. Over areas with both ice and water the influence of open water roughness on the Tb's and the ice emissivity is scaled linearly with the ice

concentration. The emissivity of ice is given by standard tie-point emissivities. The correction procedure is described in detail in Andersen et al. (2006B). The NWP model grid points are co-located with the satellite swath data in time and space and a correction to the Tb's using Eq. 1 is applied. ECMWF ERA 40 data are used for the period from 1978 to 2002, and ECMWF data from the operational model are used from 2002 onwards. A description of the ERA 40 data archive and the reprocessing can be found in Kålberg et al. (2004). These two NWP model data sets are not completely consistent, however the inconsistencies are expected to be small and the residual error is included in the error estimate.

The representation of atmospheric liquid water column (L) in the NWP data is not suitable to use for Tb correction (see Andersen et al., 2006B). The Tb's are therefore not corrected for the influence of L. Assuming neutral atmospheric conditions, the wind speed at 10 m, given by the NWP model, is converted to the surface friction velocity using the factor 0.047. The other NWP variables are used directly.

3. Algorithms

This chapter gives a scientific description of the algorithms that have been used in the reprocessing, and how the reprocessing setup differs from the operational OSI SAF algorithm.

3.1 The ice concentration algorithm

A set of three different ice concentration algorithms were applied to reprocess the satellite microwave radiometer data record from 1978 to 2007. The three ice concentration algorithms are the TUD (Technical University of Denmark) using the high resolution and high frequency channels on the SSM/I from 1991 and onwards (Andersen et al., 2006B), the Bootstrap algorithm in frequency mode (Comiso, 1986; Comiso et al., 1997), and the Bristol algorithm (Smith, 1996). The latter two are used in combination as a hybrid algorithm, which uses the near 18 and 37 GHz channels from the SMMR and SSM/I instruments since 1978.

3.1.1 Selection of algorithm

When selecting an ice concentration algorithm it is important to ensure low sensitivity to the error sources, including variability in atmospheric emission and surface emission. It is particularly important to find low sensitivity to the parameters which are not properly corrected for by (using auxiliary data), such as cloud liquid water in the atmosphere and for ice surface emissivity variability. For climate time series it is important to find an algorithm using the 19 and 37 GHz channels which can be used as far back in time as possible, including the SMMR period from 1978 to 1987 and the first SSM/I (F8) from 1987 to 1991. The SMMR did not have near 90 GHz radiometers and the 85 GHz radiometer on F8 was not functional. The 85 GHz radiometer was only used for internal use during the SSM/I period.

The analysis of atmospheric sensitivity in Andersen et al. (2006B) showed that the Bootstrap frequency mode algorithm (Comiso, 1986) had the lowest sensitivity to atmospheric noise over open water. Furthermore, the comparison to high resolution SAR imagery in Andersen et al. (2007) revealed that among the algorithms using the low frequency channels (18 and 37 GHz), the Bristol algorithm (Smith, 1986) had the lowest sensitivity to ice surface emissivity variability. In addition this algorithm had a low sensitivity to atmospheric emission in particular at high ice concentrations.

Consequently, a hybrid algorithm has been established as a linear combination of two of the tested algorithms, the Bristol algorithm and the Bootstrap frequency mode algorithm. To ensure an optimum performance over both marginal and consolidated ice, and to retain the virtues of each algorithm, the Bristol algorithm is given little weight at low concentrations, while the opposite is the case over high ice concentrations.

3.1.2 The hybrid ice concentration algorithm

The Bootstrap algorithm (Comiso, 1986) is based on the observation of linear clustering of ice Tb's in scatter plots of T_{37v} vs T_{19v} whereas open water Tb's cluster around a single point. It assumes only two surface types: ice and open water, taking into account the variability of both to optimize the detection of small sea ice concentrations. The linear relationship yields the following simple formulation for the total ice concentration, Ct:

$$Ct = (Tb - Tb^W)/(Tb^I + Tb^W) \quad , \qquad \text{(Eq. 2)}$$

where Tb is the measured brightness temperature, Tb^W is the open water tie point, and Tb^I is the ice tie point (see section 3.2).

The Bristol algorithm (Smith, 1996) is conceptually similar to the Bootstrap algorithm. In a three-dimensional scatter plot spanned by T_{19v}, T_{37v} and T_{37h} the ice Tb's tend to lie in a plane. The only difference to the Bootstrap algorithm is that instead of viewing the data in the T_{19v}, T_{37v} space, the Bristol algorithm views the data perpendicular to the plane in which the data lies, i.e. in a transformed coordinate system:

$$1. axis: T_{37v} + 1.045 T_{37h} + 0.525 T_{19v} \quad , \qquad \text{(Eq. 3a)}$$

$$2. axis: 0.9164 T_{19v} - T_{37v} + 0.4965 T_{37h} \quad . \qquad \text{(Eq. 3b)}$$

The remaining analysis is identical to the Bootstrap algorithm.

The Bootstrap algorithm is used over open water and the Bristol algorithm is used over ice. At intermediate concentrations up to 40% the ice concentration is an average weighted linearly between the two algorithms, as shown in Eq. 3c and 3d. This hybrid algorithm is the OSI SAF sea ice concentration algorithm.

$$iceconc = (1 - wc) * conc_{bristol} + wc * conc_{bootstrap} \quad , \qquad \text{(Eq. 3c)}$$

$$wc = (\|(t - conc_{bootstrap})\| + t - conc_{bootstrap}) / (2 * t) \quad , \qquad \text{(Eq. 3d)}$$

where t is the threshold of 40%.

3.1.3 Tb correction for water vapor and open water surface roughness variability

Using the model function presented in 2.3, the Tb's are corrected for the influence of water vapor in the atmosphere and open water surface roughness caused by wind shear. The model function is a semi empirical radiative transfer ocean model describing the Tb as a function of sea surface temperature, surface wind friction velocity, total atmospheric water vapor, total cloud liquid water and surface air temperature. The model function used for SMMR processing is described in Wentz (1983) and the one used for SSM/I processing is described in Wentz (1997). The correction procedure is described in Andersen et al. (2006B). At intermediate ice concentrations the surface emission term is a linear combination of ice emissivity derived from tie-point signatures and the open water emissivity derived from the model. The total ice concentration is solved by iteration.

3.2 Dynamical tie-points

Tie-points are typical signatures of 100% ice and open water which are used in the ice concentration algorithms as a reference. The tie-points are derived by selecting Tb's from regions of known open water and 100% ice. Usually these tie-points are static in time and space, but they can be adjusted to follow the seasonally changing signatures of ice and open water as it is currently done in the operational OSI SAF ice concentration processing. Static tie-points are prone to be affected by sensor drift, inter sensor calibration differences and climatic trends in surface and atmospheric emission. The data must therefore be carefully calibrated before computing the ice concentrations. Here we use dynamic tie-points, a method that minimizes these unwanted effects, with or without prior calibration.

During winter, in the consolidated pack ice well within the ice edge, the ice concentration is very near 100 % (Andersen et al., 2007). This has been established using high resolution SAR data, ship observations and by comparing the estimates from different ice concentration algorithms. The apparent fluctuations in the derived ice concentration in the near 100% ice regime are primarily attributed to snow/ice surface emissivity variability around the tie-point signature and only secondarily to actual ice concentration fluctuations. In the marginal ice

zone the atmospheric emission may be significant. The fluctuations due to atmospheric and surface emission are systematic. In fact, different algorithms with different sensitivity to atmospheric and surface emission compute very different trends in sea ice area on seasonal and decadal time scales (Andersen et al., 2007). This means that not only do the sea ice area have a climatic trend, but the atmospheric and surface constituents affecting the microwave emission are also changing. For example, different wind patterns, water vapor and liquid water concentrations in the atmosphere, snow depth, fraction of perennial ice etc. In an attempt to compensate for the influence of these unwanted trends the tie-points are derived dynamically using a monthly mean around the reprocessing point in time. It is assumed that ice concentrations from the NASA Team algorithm above 95 % are in fact near 100 % ice and that the mean value of these data points can be used to derive the ice tie-point (for SMMR NASA team tie-points from Gloersen et al. (1992) were used and for SSM/I tie-points from Andersen (1999) were used). The NASA Team ice concentration is the initial guess before the iteration and the OSI SAF ice concentration does not depend on the NASA Team ice concentration. The analysis of SAR data in Andersen et al. (2007) from the central arctic showed that during winter there is more than 99% ice cover. During strong ice drift divergence and during the summer there may situations where this is not the case. However, during one month of tie-point data collection we are sure to have captured the situations with near 100% ice cover. The standard deviation of the tie-point is included in the total ice concentration error estimate which is the justification for this assumption.

Geographically, the selection of data for the ice tie-point is limited by excluding regions poleward of 84°. This is due to the limited coverage of the SMMR instrument, and the same constraint has been applied to the SSM/I data for consistency. Regions of open water were used for selecting the water tie-point data (53N to 75N and 65S to 80S). There is no attempt to compensate explicitly for sensor drift or inter-sensor calibration differences between the seven different sensors used in the analysis. The dynamical tie-point method is in principle compensating for these problems in a consistent manner.

3.3   Sea ice concentration uncertainties

Uncertainty estimates are needed when the ice concentration data are compared to other data sets or when the ice concentrations are assimilated into numerical models. The uncertainties are computed for each data point and are not interpolated or filled into regions with no data. The uncertainty is given in terms of one standard deviation and quantifies the confidence we have in a certain data point. The uncertainty scales with the weighting given each observation when assimilated in models. The overall accuracy of the SMMR total ice concentrations are estimated to be ±7% (Gloersen et al., 1992). The mean accuracy of some of the more common algorithms, used to compute ice concentration from SSM/I data, such as NASA Team and Bootstrap are reported to be 1-6 % in winter (Andersen et al., 2006A).

The polar atmosphere is generally transparent for microwave radiation in between the sounding channels called the atmospheric windows near 18, 36, 90, and 150 GHz. For typical polar atmospheric states the down-welling emission at the surface is about 5-15 K at 18 GHz, 20-40 K at 36 GHz, 30-100 K at 90 GHz. For comparison, the sea ice surface emission is typically 150-260 K. When computing the ice concentration using the atmospheric window channels, the atmospheric emission and scattering is an error source. The tie-points are typical ice and water signatures representative on a hemispheric scale. Deviations from the typical surface emission signatures result in ice concentration uncertainties. Both the SMMR and the SSM/I instruments have large foot-prints on the ground, and the algorithms with the lowest sensitivity to both atmospheric and surface emissivity variability use Tb's at different frequencies with different foot-print size. Representing these large foot-prints on a finer, predefined grid results in a representativeness error. In addition there is the geo-location error, sensor noise, drift, and sea ice variability over the sampling period.

3.3.1   Error sources and definitions

The errors described in the following sections are generally independent. The tie-point uncertainty, including residual atmospheric noise, sensor noise and ice surface emissivity variability, is derived from measurements. The representativeness error is simulated.

3.3.2   Instrument errors

Random instrument noise results in Tb and ice concentration uncertainties. The SSM/I ice concentration uncertainty due to sensor noise is less than 2.6 %. The SSM/I instrument noise results in a Bristol algorithm ice concentration uncertainty of 1.4 %, 1.7 % for the Bootstrap in frequency mode (Andersen et al., 2006A).

Systematic sensor drift is in particular an important issue for ice concentration algorithms using static tie-points. Here we use dynamical tie-points intended for alleviating problems with sensor drift, inter-sensor calibration and climatic trends in ice surface emissivity and atmospheric emission, i.e. this method minimizes the uncertainties caused by sensor drift.

3.3.3   Algorithm and tie-point uncertainties

Both the water surface and ice surface emissivity variabilities result in ice concentration uncertainties. Emission and scattering in the atmosphere also affects the Tb's and the computed ice concentrations. Different algorithms have different sensitivities to these surface and atmospheric parameters (Andersen et al., 2006B). Further, both the atmospheric and surface parameters affecting the ice concentration estimates have climatic trends (Andersen et al., 2007). To minimize the uncertainties due to these two parameters, the Tb's are corrected using NWP data for atmospheric humidity and open water roughness in this reprocessing. The dynamical tie points minimize uncertainty due to the climatic trends in the atmosphere and on the ice surface on a hemispheric scale while regional trends may still exist. The remaining tie-point uncertainties are estimated from the spatial ice concentration variability in regions with open water or 100% ice.

3.3.4   Representativeness error

Foot-print sizes for the channels used for ice concentration mapping range from about 50 km for the 19 GHz channels to about 12 km for the 85 GHz channels. Foot-prints of uneven size are combined in the algorithms when computing the ice concentration. The foot-print ice concentration is represented on a predefined grid. The ice concentration data are normally represented on a finer grid (typically 12.5 or 25 km) than the sensor resolution (12 to 50 km). This is sometimes called smearing. The combination of foot-prints of uneven size in the ice concentration algorithm results in an additional smearing effect. This we call the foot-print mismatch error. The smearing and the foot-print mismatch error can not be estimated separately. However, the combined error can be estimated if all other error sources and the ice cover reference are known *a priori*. It can also be simulated using high resolution ice concentration reference data and a model for the satellite measurement foot-print patterns. In this reprocessing we use a model simulating the smearing uncertainties for different algorithms and ice concentrations (see Appendix E).

3.3.5   Geo-location error

A geo-location error occurs when the satellite is not exactly oriented. Simulations show that because the foot-prints are large compared to the typical geo-location errors (about 5km), the geo-location error is small, and therefore neglected here.

3.4 The sea ice concentration uncertainty algorithm

The detailed OSI SAF ice concentration algorithm is described in Appendix E. Below is shown examples of the derived uncertainty for an SSMI product.

Figure 1: Ice concentration from one day in September 2005 derived from SSMI data. The white areas are areas where data are not processed since climatologically they are always open water (climatology described in section 4.2.3).
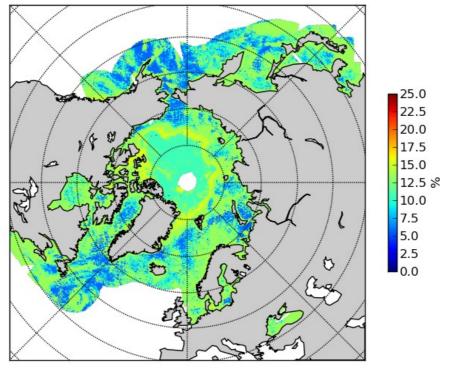

Figure 2: Total uncertainty (standard deviation) of the product shown in Figure 1.
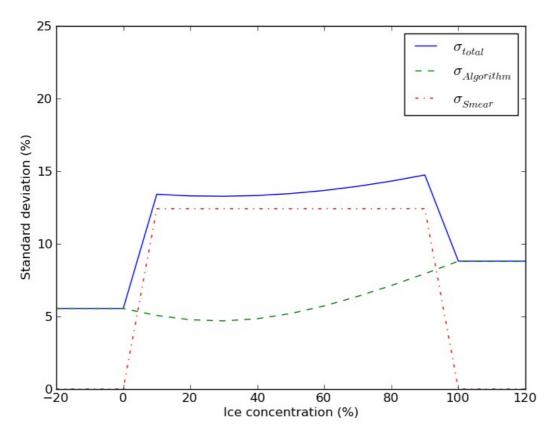
Figure 3: Total, algorithm and smear uncertainty as function of ice concentration for the product shown in Figure 1.

4. Processing scheme

This chapter describes all the processing steps in the OSI SAF sea ice concentration reprocessing scheme. The processing steps can be divided in three main steps; Level 1/2, Level 3 and Level 4. An overview of these three steps are shown in Figure 4, and the technical details are presented in more detail in the next three sections. The science behind some of these steps are discussed in Chapter 3. SMMR and SSM/I data are processed separately and not merged in the overlapping period.
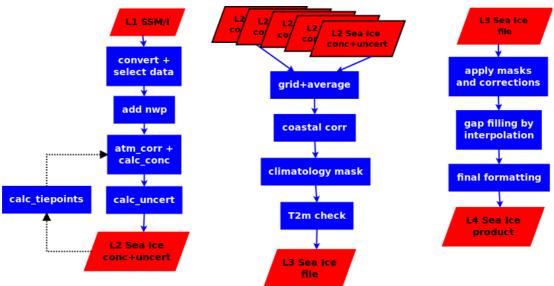

Figure 4: The three main processing elements in the ice concentration processing chain.

4.1 L1/L2 processing

This main step contains all processing done on the original swath data, without any gridding or averaging.

4.1.1 Converting antenna temperature to brightness temperature

The antenna temperatures measured by the radiometer are different from the brightness temperatures, due to antenna pattern effects such as antenna side-lobe contributions and cross polarization coupling (Njoku et al. 1980; Njoku, 1980). The SSM/I data provided by the RSS are converted from antenna temperatures to brightness temperatures using the method described in Wentz (1991).

4.1.2 Selection of data

The SMMR and SSM/I data sets provide almost global coverage (see also chapter 2.1 and 2.2). The exception is a circular area around each pole which is not covered due to the inclination of the satellite orbit and the limited swath width. For SMMR there are no data available poleward of 84°, and for SSM/I this limit is at 87°.

To reduce the amount of data to be processed the global data sets were filtered by selecting only data from areas where ice is ever likely to occur. For this purpose a sea ice maximum extend climatology from NSIDC has been used. Because this open water mask was close to the ice edge in certain places the open water mask has been moved 100 km further away from the ice edge. All land data more than 100km from the coast are skipped.

4.1.3 Adding NWP data

NWP data from ECMWF (see also Chapter 2.3) were interpolated in time and space to the position of each set of low resolution brightness temperatures. The following parameters were collected:

- surface temperature at 2 m height

- total column water vapor

- total column liquid water

- wind speed and wind direction at 10m height

Total column liquid water is not used in the processing, but is kept for reference.

4.1.4 RTM correction and ice concentration calculations

The NWP model grid points are co-located with the satellite swath Tb's in time and space, and a correction for water vapor and open water roughness, using Eq. 1, is applied. Over fractions of both ice and water the influence of open water roughness on the Tb's and the ice emissivity is scaled linearly with the ice concentration using iteration. The emissivity of ice is given by standard tie-point emissivities. The correction procedure is described in detail in Andersen et al. (2006B).

The ice concentration is calculated as part of the correction procedure. This gives ice concentration estimates both for uncorrected and corrected brightness temperatures. The uncorrected ice concentration estimates are only kept for reference. More details are given in Chapter 2.3 and 3.1.

4.1.5 Uncertainty calculations

The representativeness error is computed as a function of ice concentration for each algorithm and sensor using a model. The remaining error sources (including the instrument noise, residual atmospheric noise, surface emissivity noise) are estimated in combination using the hemispheric variability of the measurements. The total uncertainty is the sum of the partial uncertainties squared as described in Eq. 4. The smearing uncertainty is zero for open water and for 100 % ice. More details is given in Chapter 3.3 and Appendix E.

4.1.6 Dynamical tie-points

The L1/L2 processing is done in two steps. The two last steps are done twice, as shown in Figure 4. This is necessary for the generation of the dynamical tie-points. First, all data must be organized, a first tie-point set is generated based on uncorrected brightness temperatures and corrected brightness temperatures are calculated. Secondly, a new tie-point set is generated using the corrected brightness temperatures. With these tie-points the final ice concentration calculations are made. More details are given in Chapter 3.2.

4.2 L3 processing

This main step contains the gridding of the swath data to daily fields, and calculation of corrections and masking fields without applying these.

4.2.1 Daily gridding

The daily gridding searches for all observation within 24 hours, centered on 12:00 UTC, and grids these to the final output grid. The observations within one grid cell are averaged, using a weight defined as:

$$ \text{,} \qquad \text{(Eq. 5)} $$

where *dist* is the distance between the observation and center of grid point, and *inflrad* is the radius of influence. The influence radius depends on the sampling radius for the channel. For low resolution channels (19, 22 and 37 GHz) 18 km is used and for 85GHz 9 km is used. The 85GHz is kept for internal use, and no ice concentration product based on this sensor is provided.

The gridding is done for all areas with data coverage, including the coastal zone. A gridded field is made for all the ice concentration estimates, based on both uncorrected and corrected brightness temperatures, and for the algorithms present in the L2 files. A similar gridding/averaging is applied for the uncertainty estimates.

In the averaging, observations from multiple satellite missions are available in overlapping periods. During overlaps in the SSM/I period, observations from different satellites are averaged. The dynamical tie-point approach handles the possible inter satellite differences, which is shown in the validation report [RD.2]. Data during the overlap period between SMMR and SSM/I data are not mixed, as these instruments are more different.

4.2.2 Coastal correction

Observations in the coastal zone are a mixture between land and water/sea ice. Land has similar signatures to sea ice, and the algorithms therefore overestimate the sea ice concentration in these areas. To correct for these so-called land spill-over effects, an extra coastal correction step has been implemented. The method implemented is described in detail in Cavalieri et al. (1999). In short, this method first calculates monthly average ice concentration for all the months in a selected year and then finds the minimum ice concentration from these averages. This minimum is then used to correct the ice concentration values in the coastal zone if adjacent non-coastal grid points are ice free. The minimum monthly average ice concentration fields were calculated using data from 1985 for SMMR and 1992 for SSM/I. Separate fields were calculated for all algorithms processed.

This processing step generates an additional field with the coastal correction to be added to the concentration field, without applying it.

4.2.3 Climatological maximum extent masking

To mask out erroneous ice outside areas where sea ice is ever likely to occur, a monthly maximum extent climatology has been used. This climatology has been produced by NSIDC using SMMR and SSM/I monthly averaged ice concentrations and finding the maximum extent for each month between 1979 and 2007. A zone of 100 km has been added to the maximum extent NSIDC maps to assure that the masks are surely outside the areas were sea ice is ever likely to occur. Examples of these masks are given in Appendix B. More details about these monthly climatological maximum fields (or ocean mask as called by NSIDC) are available from NSIDC:

http://nsidc.org/data/smmr_ssmi_ancillary/ocean_masks.html.

This processing step collects the respective monthly mask and adds it to the file as a separate layer.

4.2.4 T2m check

A quality check using the NWP T2m (air temperature at 2 meters) field is used in the processing. The T2m NWP values that have been interpolated in time and space to each observation in the add NWP step, are gridded and averaged to the product grid similar as for the ice concentrations. This field is then added as a separate layer for later use. The test applying the T2m value is based on experience from the operational OSI SAF chain, and shows useful for removing gross errors far from the sea ice edge. In the reprocessing data set it is not used for modifying the nominal value, just mark questionable data.

4.3 L4 processing

This final main step contains filling of some areas with missing data by interpolation and applying masks and corrections to present the final ice concentration product. The processing flag variable (section 5.1.3) is computed during these steps.

4.3.1 Applying masks and coastal correction

A sea ice concentration analysis step is performed. It deals with applying the various masking steps, the coastal correction and the T2m check (as described in sections 4.2.2, 4.2.3 and 4.2.4) are applied.

The nominal values of the ice concentrations and uncertainties are modified (except the T2m test), and a variable holding the processing flags is created. The flags are described in section 5.1.3.

4.3.2 Gap filling by interpolation

For easing the use of the reprocessing data set, it was decided that some level of spatial interpolation should be performed for reducing the occurrence of gaps. Only missing data are interpolated. Interpolated data points are clearly marked in the product file (section 5.1.3) so that users can choose to discard them and only ingest retrievals that rely on satellite signal.

Data gaps can occur in several forms, such as missing scan lines, missing orbits and polar observation hole. While spatial interpolation might be efficient in filling small gaps (e.g. one or two missing scan lines), it necessarily blurs the sea ice concentration features. This effect becomes overwhelming when large areas are missing. To overcome this issue, yet implementing a general approach for all cases, the ice concentration estimates from the previous and next daily products are used in the interpolation as well. In the case of SSM/I, it means that interpolation on a given date D uses pixels from 3 data files: D-1, D and D+1.

The interpolated value at grid cell (i,j) for day *D* is given by:

$$X_{i,j}^{D} = K \cdot \left(w_{i,j}^{D-1} \cdot X_{i,j}^{D-1} + w_{i,j}^{D+1} \cdot X_{i,j}^{D+1} + \sum_{k,l} W^{D}(k,l;i,j) X_{k,l}^{D} \right) \quad \text{(Eq. 6)}$$

where *X* is the sea ice concentration value and *K* is a normalizing factor given by:

$$w_{i,j}^{D-1} + w_{i,j}^{D+1} + \sum_{k,l} W^{D}(k,l;i,j) = 1/K \quad .$$

From Eq. 6, it is clear that the *spatial* interpolation from neighbors of cell (i,j) only uses values from date *D*, while the *temporal* interpolation is only concerned with the value from the exact (i,j) cell but from dates *D-1* and *D+1*. This strategy ensures that the interpolation will be efficient in the two following extreme scenarios. In a region where we never have satellite observations (e.g. the polar observation hole in the Northern Hemisphere), the spatial interpolation term will be the only contribution. Conversely, in the case of several missing swath on date D only (nominal coverage on D-1 and D+1), the interpolated values will be computed from the previous and next dates, taking advantage of the persistence of sea ice concentration over such a short period. The interpolation for intermediate cases (when both spatial and temporal neighbors exist) is a compromise of those extreme situations.

In Eq. 6, the weighting parameters are computed as follows:

$$w_{i,j}^{D} = 1/(\sigma_{i,j}^{D})^{2} \cdot (2 N_{max} + 1)$$

$$W^{D}(k,l;i,j) = 1/(\sigma_{k,l}^{D})^{2} \times \exp\left(-0.5 \cdot \left(\frac{\Delta(k,l;i,j)}{R_{i,j}}\right)^{2}\right) \quad , \quad \text{(Eq. 7)}$$

where σ is the standard deviation associated to each ice concentration estimate (section 3.3), Δ is the distance between a given (k,l) neighbor and cell (i,j) and R is an auto-correlation radius. The spatial interpolation weight is thus based on an isotropic gaussian shape, and almost all (>99.9%) of the interpolation weight is concentrated inside a [-3R;+3R] x [-3R;+3R] km^2 area, which translates into a [$-N_{max}$;+N_{max}] x [$-N_{max}$;+N_{max}] grid cells square area. It was found that a spatially varying radius R was needed for optimal gap filling and the value R = latitude of (i,j) (in degrees) was taken.

In the case of SMMR which was operated every second day, the interpolation is performed with *D-2* and *D+2* instead of *D-1* and *D+1*.

4.3.3 Final formatting

This step is only concerned with the final formatting of the data sets into a CF compliant NetCDF file. This implies selection of a limited number of variables (ice concentration, uncertainties, processing flags, latitude, longitude) for the selected algorithm and extraction to a new file where global attributes are added. The format of this product file is described in the next chapter.

Since SMMR and SSM/I are processed separately, there is a period with overlapping products in July and August 1987. The quality is better for the SSM/I and should be preferred during the overlapping period.

5. Product description

This chapter gives a description of the product specification, meta data, data format and product availability.

5.1 Product specification

The product consists of three major fields:

- sea ice concentration
- uncertainty estimate
- processing flag

The definitions of these three fields are given in the sections below. These fields are given in the same grid.

5.1.1 Sea ice concentration

Sea ice concentration indicates the areal fraction of a given grid point covered by ice. It is given as a real number in percentage, with a range from 0-100%.

5.1.2 Uncertainty estimate

An estimate of the uncertainty of each sea ice concentration value is given in a separate field. The uncertainty is given as standard deviation in percentage, with at range from 0-100%.

5.1.3 Processing flag

The processing flag contains information about the processing steps that have influenced the ice concentration value. It is coded as a signed character, with one flag value for each ice concentration value. The different values are described in Table 4. These flags are not additive, so all the values are exclusive (e.g. coastal correction and gap filling can not occur for the same data point).

Value	Quality indication	Definition
0	Nominal	Nominal ice concentration value given.
1	Nominal value questionable	Nominal value, but T2m check indicates possibility of false ice due to high surface air temperature (> +10°C).
2		Nominal value, but quality questionable because of lake ice.
10	Nominal value changed	Coastal correction has been applied.
11		Climatological maximum extent mask has been applied inside data area.
12		As value 11, but outside of data coverage area.
13		Gap filling has been applied.
100	Missing value	Missing value due to land.
101		Missing value due to missing data.

Table 4: Definition of sea ice concentration processing flags.

5.2 Grid specification

The sea ice concentration product is available on two projections and grids, each with one product for each hemisphere. The projections used are a Lambert Azimuthal Equal Area projection with grid a resolution of about 12.5 km, and a Polar Stereographic projection with a grid resolution of 10.0km. The Lambert grid is also called the EASE grid, and it is used by NSIDC for several of their sea ice products. More documentation about the EASE grid can be found on their web site: http://nsidc.org/data/ease/.

The details of the grid definitions are given in Table 5 and Table 6 below. Maps of the areas are shown in Figure 5 and Figure 6. Projection definitions in the form of PROJ-4 initialization strings are also given (see [http://www.remotesensing.org/proj] for details).

Projection:	Lambert Azimuthal Equal Area
Resolution:	12.5337625 km
Size:	849 columns, 849 lines
Central Meridian:	0°
Radius of Earth:	Spherical: 6371228.0 m
PROJ-4 string:	NH: +proj=laea +R=6371228.0 +lat_0=90 +lon_0=0 SH: +proj=laea +R=6371228.0 +lat_0=-90 +lon_0=0

Table 5: Geographical definition for the EASE 12.5 km grid, Northern and Southern Hemisphere.

Projection:	Polar Stereographic
Resolution:	10.0 km
Size:	NH: 860 columns, 1120 lines SH: 790 columns, 830 lines
Central Meridian:	-45°
Radius of Earth:	Elliptical: a=6378273.0m , b=6356889.44891 m
PROJ-4 string:	NH: +proj=stere +a=6378273 +b=6356889.44891 +lat_0=90 +lat_ts=70 +lon_0=-45 SH: +proj=stere +a=6378273 +b=6356889.44891 +lat_0=-90 +lat_ts=-70 +lon_0=0

Table 6: Geographical definition for the Polar Stereographic 10.0 km grid, Northern and Southern Hemisphere.

5.3 Meta data specification

The meta data included in the product file are given as NetCDF attributes to the variables and to the file (Global Attributes). Attributes associated to the variables are those required by the CF convention. The Global Attributes have been selected for matching requirements from the International Polar Year projects DAMOCLES and iAOOS-Norway (http://dokipy.met.no). GCMD and IMO keywords were also selected. An ASCII version of the NetCDF header, as given by `ncdump,` is given in Appendix A.
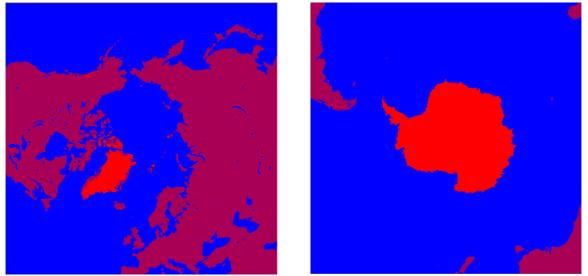
Figure 5: Area covered by the EASE 12.5 km grids for Northern (left) and Southern (right) hemispheres.
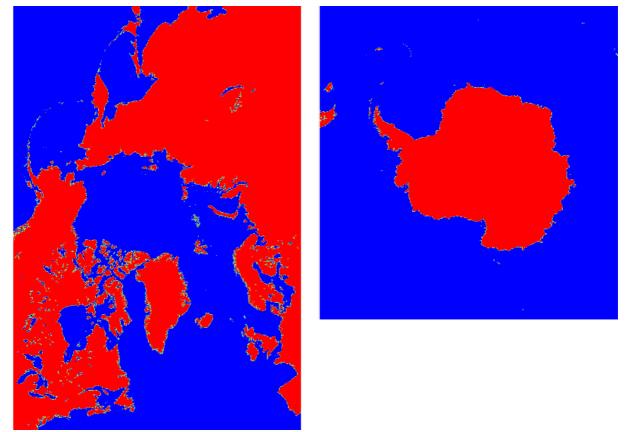

Figure 6: Area covered by the Polar Stereographic 10.0 km grids for Northern (left) and Southern (right) hemispheres.

5.4 File naming convention

The NetCDF product file have the following naming convention:

```
ice_conc_<area>_<proj>-<gridRes>_reproc_<date12>.nc ,
```

where:

`<area>` : `<nh>` (Northern Hemisphere) and `<sh>` (Southern Hemisphere)

`<proj>` : `<ease>` for the equal area Lambert azimuthal projection, `<polstere>` for the Polar Stereographic projection.

`<gridRes>` : spatial resolution of the grid (`<125>` for 12.5 km, `<100>` for 100 km)

`<date12>` : central date of the analysis `<YYYYMMDD1200>`, e.g. 199112021200.

5.5 Product availability

The OSI SAF sea ice concentration reprocessing data set covers the period from 26.10.1978 to 23.10.2009. Some dates are missing due to lack of satellite data. These dates are listed in Appendix C.

The data set is distributed freely through the OSI SAF Sea Ice FTP server, available at this address:

ftp://saf.met.no/reprocessed/ice/conc/v1p1/

The data are organized in year and month directories. The SMMR data covers the period from from 26.10.1978 to 09.07.1987 and the SSM/I data covers the period from 10.07.1987 to 23.10.2009. The overlapping SMMR data (11.07.1987 – 20.08.1987) are made available for reference, and kept in the directory called "overlapping_smmr".

5.6 Delivery of updates

The current version covers the period from 1978 to 2009. A continuation of this reprocessing effort is planned. A service with monthly updates is expected in the OSI SAF CDOP-2 phase at end of 2012.

6.　References

Andersen, S., L. Toudal Pedersen, G. Heygster, R. Tonboe, and L Kaleschke, Intercomparison of passive microwave sea ice concentration retrievals over the high concentration Arctic sea ice. *Journal of Geophysical Research* 112, C08004, doi10.1029/2006JC003543, 2007.

Andersen, S., R. T. Tonboe and L. Kaleschke. Satellite thermal microwave sea ice concentration algorithm comparison. *Arctic Sea Ice Thickness: Past, Present and Future*, edited by Wadhams and Amanatidis. Climate Change and Natural Hazards Series 10, EUR 22416, 2006A.

Andersen, S., R. Tonboe, S. Kern, and H. Schyberg. Improved retrieval of sea ice total concentration from spaceborne passive microwave observations using Numerical Weather Prediction model fields: An intercomparison of nine algorithms. *Remote Sensing of Environment104, 374-392*, 2006B.

Cavalieri, D.J., C.L. Parkinson, P. Gloersen, J.C. Comiso, and H.J. Zwally. Deriving long-term time series of sea ice cover from satellite passive-microwave multisensor data sets. *Journal of Geophysical Research* 104(C7), 15803-15814, 1999.

Comiso J.C, D.J. Cavalieri, C.L. Parkinson, and P. Gloersen. Passive microwave algorithms for sea ice concentration: A comparison of two techniques. *Remote Sensing of Environment* 60, 357-384, 1997.

Comiso J.C. Characteristics of arctic winter sea ice from satellite multispectral microwave observations. *Journal of Geophysical Research* 91(C1), 975-994, 1986.

Gloersen, P., and F. T. Barath. A scanning multichannel microwave radiometer for Nimbus-G and SeaSat-A. *IEEE Journal of Oceanic Engineering OE-2*(2), 172-178, 1977.

Gloersen, P., W. J. Campbell, D. J. Cavalieri, J. C. Comiso, C. L. Parkinson, H. J. Zwally. Arctic and Antarctic sea ice, 1978-1987: satellite passive-microwave observations and analysis. *NASA SP-511*, Washington D. C., 1992.

Kållberg, P., A. Simmons, S. Uppala, and M. Fuentes. The ERA-40 archive. *ERA-40 Project Report Series*, ECMWF, Reading, 2004.

Meier, W. Scanning Multichannel Microwave radiometer (SMMR) reprocessing for EUMETSAT. *OSI SAF Visiting Scientist Report*. 9 pages, 2008.

Njoku, E. G. Antenna pattern correction procedures for the scanning multichannel microwave radiometer (SSMR). *Boundary Layer Meteorology 18*, 78-98, 1980.

Njoku, E. G., E. J. Christensen, and R. E. Cofield. The Seasat scanning multichannel microwave radiometer (SMMR): Antenna corrections - development and implementation. *IEEE Journal of Oceanic Engineering OE-5(*2), 125-137, 1980.

Smith, D. M. Extraction of winter sea ice concentration in the Greenland and Barents Seas from SSM/I data. *International Journal of Remote Sensing 17*(13), 2625-2646, 1996.

Stark, J. (2008) Sea ice reanalysis using the OSI SAF sea ice processing system. *OSI SAF Visiting Scientist Report*. 39 pages.

Toudal, L. (2006) Adaptation of SAFOSI sea ice processing system to southern hemisphere. *OSISAF Visiting Scientist Report.*

Wentz, F. J. A model function for ocean microwave brightness temperatures. *Journal of Geophysical Research 88*(C3), 1892-1908, 1983.

Wentz, F. J. A well-calibrated ocean algorithm for SSM/I. *Journal of Geophysical Research* 102(C4), 8703-8718, 1997.

Wentz, F. J. User's Manual, SSM/I Antenna Temperature Tapes, Revision 1. *RSS Technical Report 120191,* 1991.

Wentz, F. J. User's Manual, SSM/I Antenna Temperature Tapes, Revision 2. *RSS Technical Report 120193,* 1993.

Wentz, F. J. User's Manual, SSM/I Antenna Temperature, Version 6. *RSS Technical Memo 082806*, 2006.
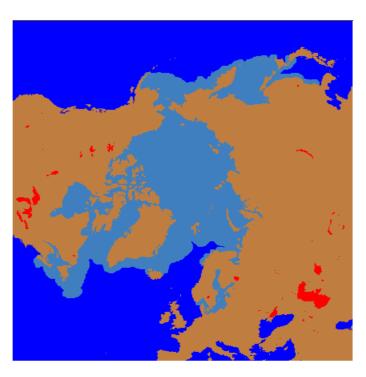
7.   Appendix A : Example of NetCDF format

Below is given an example of the NetCDF header of an OSI SAF sea ice concentration reprocessing file (CDL format).

```
netcdf ice_conc_nh_ease-125_reproc_199112021200 {
dimensions:
        time = 1 ;
        nv = 2 ;
        xc = 849 ;
        yc = 849 ;
variables:
        int Lambert_Azimuthal_Grid ;
                Lambert_Azimuthal_Grid:grid_mapping_name =
                                                "lambert_azimuthal_equal_area" ;
                Lambert_Azimuthal_Grid:longitude_of_projection_origin = 0.f ;
                Lambert_Azimuthal_Grid:latitude_of_projection_origin = 90.f ;
                Lambert_Azimuthal_Grid:false_easting = 0.f ;
                Lambert_Azimuthal_Grid:false_northing = 0.f ;
                Lambert_Azimuthal_Grid:earth_radius = 6371228.f ;
                Lambert_Azimuthal_Grid:semi_major_axis = 6371228.f ;
                Lambert_Azimuthal_Grid:proj4_string = "+proj=laea +R=6371228.0
                                                +lat_0=90 +lon_0=0" ;
        double time(time) ;
                time:long_name = "reference time of product" ;
                time:standard_name = "time" ;
                time:units = "seconds since 1978-01-01 00:00:00" ;
                time:axis = "T" ;
                time:bounds = "time_bnds" ;
        double time_bnds(time, nv) ;
                time_bnds:units = "seconds since 1978-01-01 00:00:00" ;
        double xc(xc) ;
                xc:axis = "X" ;
                xc:units = "km" ;
                xc:long_name = "x coordinate of projection (eastings)" ;
                xc:standard_name = "projection_x_coordinate" ;
                xc:grid_spacing = "12.5334 km" ;
        double yc(yc) ;
                yc:axis = "Y" ;
                yc:units = "km" ;
                yc:long_name = "y coordinate of projection (northings)" ;
                yc:standard_name = "projection_y_coordinate" ;
                yc:grid_spacing = "12.5334 km" ;
        float lat(yc, xc) ;
                lat:long_name = "latitude coordinate" ;
                lat:standard_name = "latitude" ;
                lat:units = "degrees_north" ;
        float lon(yc, xc) ;
                lon:long_name = "longitude coordinate" ;
                lon:standard_name = "longitude" ;
                lon:units = "degrees_east" ;
        short ice_conc(time, yc, xc) ;
                ice_conc:long_name = "concentration of sea ice" ;
                ice_conc:standard_name = "sea_ice_area_fraction" ;
                ice_conc:units = "%" ;
                ice_conc:_FillValue = -32767s ;
                ice_conc:valid_min = 0s ;
                ice_conc:valid_max = 10000s ;
                ice_conc:grid_mapping = "Lambert_Azimuthal_Grid" ;
                ice_conc:coordinates = "lat lon" ;
                ice_conc:scale_factor = 0.01f ;
        short standard_error(time, yc, xc) ;
                standard_error:long_name = "total uncertainty (one standard deviation)
                                of concentration of sea ice" ;
                standard_error:standard_name = "sea_ice_area_fraction
                                        standard_error" ;
                standard_error:units = "%" ;
                standard_error:_FillValue = -32767s ;
```

```
                 standard_error:valid_min = 0s ;
                 standard_error:valid_max = 10000s ;
                 standard_error:grid_mapping = "Lambert_Azimuthal_Grid" ;
                 standard_error:coordinates = "lat lon" ;
                 standard_error:scale_factor = 0.01f ;
        short algorithm_standard_error(time, yc, xc) ;
                 algorithm_standard_error:long_name = "algorithm uncertainty (one
                                     standard deviation) of concentration of sea ice" ;
                 algorithm_standard_error:standard_name = "sea_ice_area_fraction
                                                   standard_error" ;
                 algorithm_standard_error:units = "%" ;
                 algorithm_standard_error:_FillValue = -32767s ;
                 algorithm_standard_error:valid_min = 0s ;
                 algorithm_standard_error:valid_max = 10000s ;
                 algorithm_standard_error:grid_mapping = "Lambert_Azimuthal_Grid" ;
                 algorithm_standard_error:coordinates = "lat lon" ;
                 algorithm_standard_error:scale_factor = 0.01f ;
        short smearing_standard_error(time, yc, xc) ;
                 smearing_standard_error:long_name = "smearing uncertainty (one
                                     standard deviation) of concentration of sea ice" ;
                 smearing_standard_error:standard_name = "sea_ice_area_fraction
                                                   standard_error" ;
                 smearing_standard_error:units = "%" ;
                 smearing_standard_error:_FillValue = -32767s ;
                 smearing_standard_error:valid_min = 0s ;
                 smearing_standard_error:valid_max = 10000s ;
                 smearing_standard_error:grid_mapping = "Lambert_Azimuthal_Grid" ;
                 smearing_standard_error:coordinates = "lat lon" ;
                 smearing_standard_error:scale_factor = 0.01f ;
        byte status_flag(time, yc, xc) ;
                 status_flag:long_name = "status flag for sea ice concentration
                                                            retrieval" ;
                 status_flag:standard_name = "sea_ice_area_fraction status_flag" ;
                 status_flag:_FillValue = -128b ;
                 status_flag:valid_min = 0b ;
                 status_flag:valid_max = 101b ;
                 status_flag:grid_mapping = "Lambert_Azimuthal_Grid" ;
                 status_flag:coordinates = "lat lon" ;
                 status_flag:flag_values = 0b, 1b, 2b, 10b, 11b, 12b, 13b, 100b, 101b ;
                 status_flag:flag_meanings = "nominal t2m lake coastcorr maxclim_change
                                     maxclim_set interpolated land missing" ;
                 status_flag:flag_descriptions = "\n",
                     "  0 -> nominal value from algorithm used\n",
                     "  1 -> t2m check indicates possibly false ice\n",
                     "  2 -> over lake caused possibly less accurate\n",
                     " 10 -> value changed by coast correction method\n",
                     " 11 -> value changed by applying maximum climatology\n",
                     " 12 -> missing value set by applying maximum climatology\n",
                     " 13 -> value set by applying interpolation\n",
                     "100 -> missing value due to over land\n",
                     "101 -> missing value due to missing data" ;

// global attributes:
                 :title = "OSI SAF Global Reprocessed Sea Ice Concentration" ;
                 :product_id = "OSI-409" ;
                 :product_name = "osi_saf_ice_conc_reproc" ;
                 :product_status = "offline" ;
                 :abstract = "The reprocessing of sea  ice  concentration  is  obtained
                                                                         from\n",
                     "passive microwave satellite data over the polar  regions.
                                                                         It\n",
                     "is based on atmospherically corretected signal and an
                                                                         optimal\n",
                     "sea ice concentration algorithm. This  product  is
                                                                     available\n",
                     "for free  from  the  EUMETSAT  Ocean  and  Sea  Ice
                                                                     Satellite\n",
                     "Application Facility (OSI SAF)." ;
                 :topiccategory = "Oceans ClimatologyMeteorologyAtmosphere" ;
                 :keywords = "Sea Ice Concentration,Sea
                             Ice,Oceanography,Meteorology,Climate,Remote Sensing" ;
```

```
        :gcmd_keywords = "Cryosphere > Sea Ice > Sea Ice Concentration\n",
                "Ocean > Sea Ice > Sea Ice Concentration\n",
                "Geographic Region > Northern Hemipshere\n",
                "Vertical Location > Sea Surface\n",
                "EUMETSAT/OSISAF > Satellite Application Facility on Ocean and
 Sea Ice, European Organisation for the Exploitation of Meteorological Satellites" ;
        :northernmost_latitude = 90.f ;
        :southernmost_latitude = 17.71581f ;
        :easternmost_longitude = 180.f ;
        :westernmost_longitude = -180.f ;
        :activity_type = "Space borne instrument" ;
        :area = "Northern Hemisphere" ;
        :start_date = "1991-12-02 00:00:00" ;
        :stop_date = "1991-12-03 00:00:00" ;
        :project_name = "EUMETSAT OSI SAF" ;
        :institution = "EUMETSAT OSI SAF" ;
        :PI_name = "Rasmus Tonboe and Steinar Eastwood" ;
        :contact = "osisaf-manager@met.no" ;
        :distribution_statement = "Free" ;
        :references = "Global Sea Ice Concentration Reprocessing Product User
                Manual, Tonboe and Eastwood (editors), v1.1, October 2011\n",
                "http://saf.met.no\n",
                "http://www.osi-saf.org" ;
        :history = "2010-01-13 creation" ;
        :product_version = "1.0" ;
        :software_version = "4.0" ;
        :netcdf_version = "3.6.3" ;
        :Conventions = "CF-1.4" ;
}
```

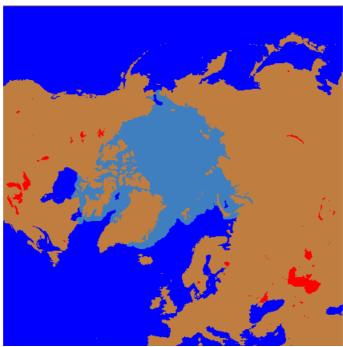# 8. Appendix B: Examples of monthly climatological maximum extent masks

Figure 7: Climatological maximum sea ice extent during March (upper) and September (lower)

9. Appendix C: Missing dates

The reprocessing data set covers the period from 26.10.1978 to 23.10.2009. During the SMMR period only every second day is available. The SMMR data have been used until 11.07.1987. SMMR data are missing during November and December 1980, in addition to shorter periods. Table 7 below lists the dates with no product due to lack of satellite data, except the expected missing SMMR days (every second day).

Year	Missing dates
SMMR	
1979	*21/5-27/5*
1980	*4/1-10/1, 27/2-4/3, 16/3-21/3, 9/4-15/4, 1/11-31/12*
1981	*27/2-5/3*
1982	*14/7-16/7, 30/7-1/8, 3/8-5/8, 15/8-17/8*
1984	*12/8-24/8*
1985	*22/9-28/9*
1986	*29/3-3/4, 5/4-9/4, 21/5-25/5, 27/5-6/6, 8/6-16/6, 8/12-10/12, 16/12-18/12*
1987	*3/1-15/1, 7/4-9/4*
SSM/I	
1987	25/08-26/08, 06/10-07/10, 03/12-31/12
1988	01/01-21/01, 06/05-08/05, 23/09, 25/12-27/12
1989	07/06, 23/07-24/07, 23/10
1990	13/08, 25/08-26/08, 21/10-22/10, 26/10-28/10, 22/12-26/12
1992	18/06
1993	04/01
1994	20/07, 20/11-21/11
2000	01/12

Table 7: Dates with no reprocessing product due to lack of satellite data. SMMR (25.10.1978-20.08.1987) was operated every second day and the table shows the periods with missing SMMR data for more than two days.

10. Appendix D: Metadata List for EUMETSAT Data Center

The EUMETSAT Data Center metadata parameters [RD.6] applicable to the reprocessed OSI SAF Sea Ice Concentration product are listed in Table 8. These metadata parameters are available in XML formatted files, one for each product file. These XML metadata files are available through the EUMETSAT Data Center.

Short Name	Attribute Name	Notes
AAAR	Geographic Area	'NH' or 'SH'
AARF	Archive Facility	UMARF
AIID	Instrument ID	'SSM/I' or 'SMMR'
APAS	Product Actual Size	In bytes
APNM	Product Type	OSICOGBRE
ASTI	Satellite ID	Nimbus, F-08, F-10, F-11,F-13, F-14 or F-15
AVBA	Base Algorithm Version	
AVPA	Product Algorithm Version	
GDMD	Disposition Mode	O = Operational
GGTP	Granule Type	DP = Data Product
GNFV	Native Product Format Version	
GORT	Orbit Type	LEO
GPLV	Processing Level	O3
GPMD	Processing Mode	O = Offline
PPRC	Processing Center	OSNMI
PPST	Processing End Date and Time	
QQOV	Overall Quality Flag	'OK' or 'NOK'
SNIT	Reference Time	
SSBT	Sensing Start Date and Time	
SSST	Sensing End Date and Time	

Table 8: EUMETSAT Data Center metadata parameters applicable to the reprocessed OSI SAF Sea Ice Concentration product.
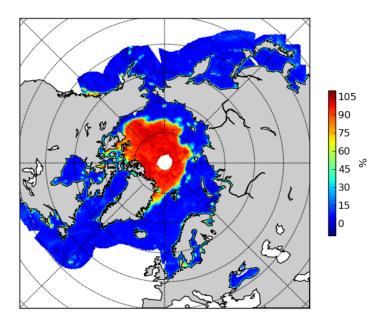
Figure 8: Ice concentration September 2005 derived from one day of SSMI data

11 Appendix E: Ice concentration uncertainties

The uncertainties are calculated based on all the swath pixels contributing to a level 3 ice concentration product (see figure 8).

11.1 Uncertainty implementation

We make the assumption the total uncertainty σ_{tot} can be written as

$$\sigma_{tot}^2 = \sigma_{algo}^2 + \sigma_{smear}^2 \tag{1}$$

where σ_{algo} is the inherent uncertainty of the concentration algorithm, σ_{smear} is the uncertainty due to resampling to a grid where the sensor footprint covers more than one pixel.

11.1.1 Algorithm uncertainty

Ice concentration can be interpreted as a superposition of water and ice

$$ice_{conc} = (1 - \alpha(ic)) \cdot water + \alpha(ic) \cdot ice \tag{2}$$

where ic is the ice concentration calculated by the algorithm.
The functional dependency between α and the calculated ice concentration ic is described by:

$ic \leq 0$	$\alpha = 0$
$0 < ic < 1$	$\alpha = ic$
$ic \geq 1$	$\alpha = 1$

which can be written as

$$\alpha(ic) = \Pi_{0,1}(ic)ic + H(ic - 1) \tag{3}$$

where $\Pi_{a,b}(x)$ is the Boxcar function and $H(x)$ the Heaviside step function. Using equation 2 and assuming the uncertainty for the ice and water part is independant this leads to a total algorithmic uncertainty as

$$\sigma_{algo}(\alpha(ic)) = \sqrt{(1 - \alpha(ic))^2 \sigma_{water}^2 + \alpha^2(ic)\sigma_{ice}^2} \tag{4}$$

where $\sigma_{water} = \sigma(IC(P_{openwater}))$ and open water is determined by a monthly varying ocean mask, IC is the functional mapping of the ice concentration algorithm and P_C denotes the set of swath pixels for all swaths (used calculating the daily product) selected on the condition C.
$\sigma_{ice} = \sigma(IC(P_{ocean, \ nasateam>0.95}))$ e.g. the standard deviation of the calculated ice concentration of those pixels clear of the coast having a NASA Team concentration $> 95\%$.
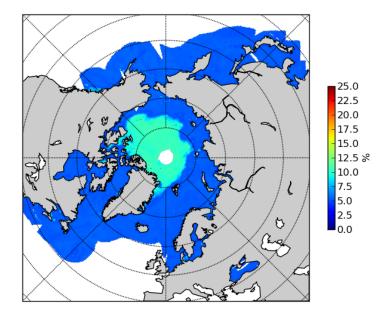An example of the algorithm uncertainty is shown in figure 9

Figure 9: Algorithm uncertainty of the ice concentration product shown in figure 8
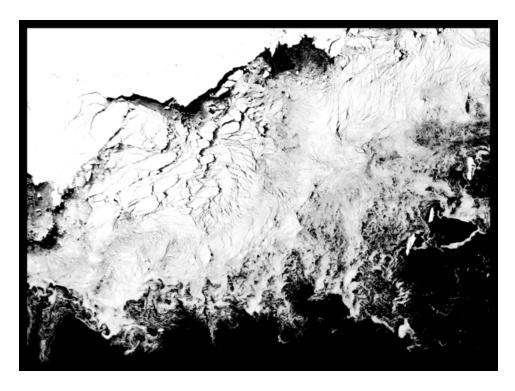
Figure 10: MODIS 1 km channel 1 image

11.1.2 Smear uncertainty

The smear uncertainty is the error due to the sensor footprint covering more than one pixel in the level3 product grid.

The error is calculated taking a cloud free 1 km MODIS image and assigning ice concentrations to all pixels based on the channel 1 brightness. For each pixel the corresponding brightness temperature is calculated for all relevant microwave channels based on standard tiepoints (Comiso et al. 1997). Using channel specific sensor footprints for weighting the ice concentration is calculated from the 1km brightness temperature image in the specified final resolution i.e. 10, 12, 25 and 50 km. This ice concentration is compared to the MODIS ice concentration regridded to the same resolution. The standard deviation of the difference between these sets of ice concentration values is the standard deviation of the smeared points.

The standard deviation of smeared points is denoted as $\sigma_{smear}(sensor, resolution, algorithm)$ (abbreviated to $\sigma_{smear}(s, r, a)$). As the ice concentration approaches zero or 1 the spatial variation of the ice cover diminishes thus the smearing has less effect. This is reflected in the
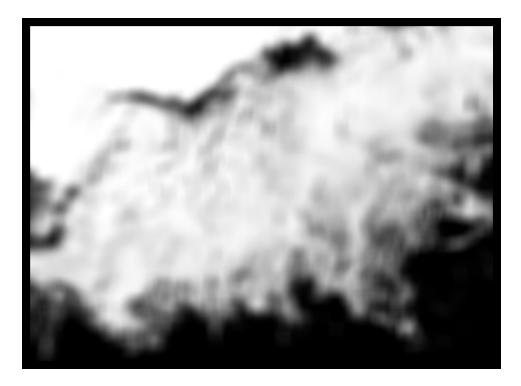
Figure 11: Resulting calculated OSI SAF ice concentration regridded to 1 km resolution

scaling:

$$
\begin{aligned}
\sigma_{ss}(s,r,a,ic) = \\
\left(\Pi_{0,\sigma_{water}}(ic)\frac{ic}{\sigma_{water}} + \Pi_{\sigma_{water},1-\sigma_{ice}}(ic) + \Pi_{1-\sigma_{ice},1}(ic)\frac{1-ic}{\sigma_{ice}} \right) \sigma_{smear}(s,r,a)
\end{aligned}
\tag{5}
$$

The use of scaling thresholds σ_{water} and $1 - \sigma_{ice}$ are somewhat arbitrarily selected.
An example of the smear uncertainty is shown in figure 12

11.1.3 OSI SAF algorithm

The OSI SAF ice concentration is calculated as a linear combination of the *Comiso* and *Bristol* algorithm which means the total smear uncertainty as

$$
ic_{osi}(ic_{comiso}, ic_{bristol}) = \left(1 - \beta(ic_{comiso})\right) ic_{comiso} + \beta(ic_{comiso}) ic_{bristol} \tag{6}
$$

where the scaling factor $\beta(ic_{comiso})$ is

$$
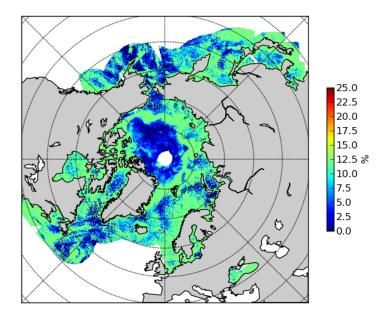\beta(ic_{comiso}) = \Pi_{0,\tau}(ic_{comiso})\frac{ic_{comiso}}{\tau} + H(ic_{comiso} - \tau) \tag{7}
$$

E-4

Figure 12: Smear uncertainty of the ice concentration product shown in figure 8

and τ a threshold value set to 0.4

11.1.4 OSI SAF uncertainty

Using equation 1 the total uncertainty is calculated as

$$\sigma_{total-osi}(s, r, osi, ic) = \sqrt{\sigma_{algo-osi}^2(ic) + \sigma_{ss-osi}^2(s, r, osi, ic)} \qquad (8)$$

An example of the smear uncertainty is shown in figure 14

11.2 Reported uncertainties

The reported uncertainties in the OSI SAF ice concentration product is the total uncertainty $\sigma_{total-osi}(s, r, osi, ic)$ (equation 8), the algorithmic uncertainty $\sigma_{algo-osi}(ic)$ (equation 4) and the smear uncertainty $\sigma_{ss-osi}(s, r, osi, ic)$ (equation 5).
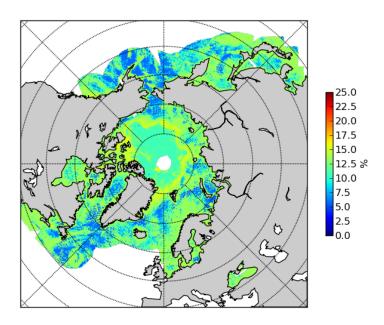
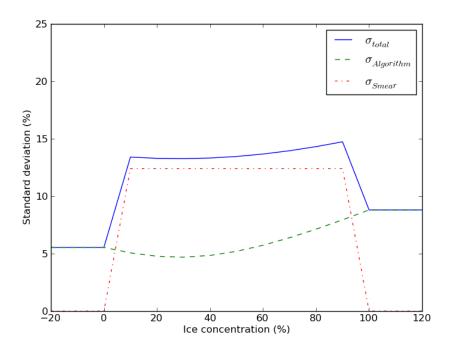Figure 13: Total uncertainty of the ice concentration product shown in figure 8

Figure 14: Uncertainty components as a function of ice concentration for the ice concentration product shown in figure 8